Analytical Methods

International Edition: DOI: 10.1002/anie.201915490
German Edition: DOI: 10.1002/ange.201915490

Molecular Fluorescence Imaging Spectroscopy for Mapping Low Concentrations of Red Lake Pigments: Van Gogh's Painting *The Olive Orchard*

*Kathryn A. Dooley, Annalisa Chieli, Aldo Romani, Stijn Legrand, Costanza Miliani, Koen Janssens, and John K. Delaney**

Abstract: *Vincent van Gogh used fugitive red lake pigments that have faded in some paintings. Mapping their distribution is key to understanding how his paintings have changed with time. While red lake pigments can be identified from micro-samples, in situ identification and mapping remain challenging. This paper explores the ability of molecular fluorescence imaging spectroscopy to identify and, more importantly, map residual non-degraded red lakes. The high sensitivity of this method enabled identification of the emission spectra of eosin (tetrabromine fluorescein) lake mixed with lead or zinc white at lower concentrations than elemental X-ray fluorescence (XRF) spectroscopy used on account of bromine. The molecular fluorescence mapping of residual eosin and two carmine red lakes in van Gogh's The Olive Orchard is demonstrated and compared with XRF imaging spectroscopy. The red lakes are consistent with the composition of paint tubes known to have been used by van Gogh.*

Introduction

Organic lake pigments, valued for their vivid colors and translucency, are made by precipitating soluble dyestuff onto an insoluble inorganic substrate or by complexation of a metal cation with a dye without a substrate.[1] Some red lake dyestuffs are naturally occurring hydroxyanthraquinones, such as alizarin or purpurin extracted from madder plants or carminic acid from insects, or synthetic derivatives such as substituted xanthenes (like found in eosin lake). The detection of lakes in paintings is an active area of research. Because some lake pigments are known to fade, determining where they have faded is important for learning about the artist's original intention and how the artwork's appearance has changed with time.

Various analytical methods can identify lake pigments. Liquid chromatography and/or mass spectrometry are the most accurate,[2–5] but require a sample. Existing imaging spectroscopy methods can identify and, more importantly, map materials across a painting. Visible-to-near-infrared (Vis-NIR) diffuse reflectance imaging spectroscopy relies on spectral features due to electronic and vibrational transitions. Insect- and plant-based red lakes are distinguishable because $S_0(\pi)\rightarrow S_1(\pi^*)$ absorption bands are spectrally shifted relative to one another.[6] X-ray fluorescence (XRF) spectroscopy can detect chemical elements and has been used to infer the presence of a lake by detecting Al, S, Ca, and Sn, amongst other elements, associated with the lake substrate.[2,3] For eosin, a brominated derivative of fluorescein, the detection of Br is a more unambiguous indication of the colorant.

Due to the molecular emission properties of red lakes, another potential mapping method is based on fluorescence. Microspectrofluorimetry has been used for lake pigment analysis on illuminated manuscripts[7] and other artworks.[8] These studies showed the need for analyzing reference paints in order to identify fluorescence spectral features characteristic of the lake. They also raised challenges when analyzing spectra from aged, solid-state samples. The fluorescence spectral shape can be distorted by self-absorption, which occurs in the spectral region where the absorption and emission spectra overlap. Fluorescence quenching can decrease the fluorescence yield and thus intensity. "Pseudo-fluorescence" also can occur when a non-emitting pigment absorbs broadband fluorescence from degraded varnishes[9,10] or paint binders. Furthermore, fluorescence from degradation products of red lake pigments can further complicate the spectral analysis.

The effects of self-absorption and pseudo-fluorescence can be removed using a Kubelka–Munk correction function that requires collecting a reflectance spectrum from the same area as the emission spectrum.[11,12] This procedure has been successful in recovering the corrected spectra of red lakes in paintings.[13,14]

The motivation for this work was to determine if molecular fluorescence imaging spectroscopy, known for its high sensitivity, could complement existing methods to

[*] Dr. K. A. Dooley, Dr. J. K. Delaney
Scientific Research Department, National Gallery of Art,
6th and Constitution Ave NW, Washington, DC 20565 (USA)
E-mail: j-delaney@nga.gov
Dr. A. Chieli, Dr. A. Romani, Dr. C. Miliani
CNR-Istituto di Scienze e Tecnologie Molecolari,
c/o Dipartimento di Chimica, Biologia e Biotecnologie,
Università di Perugia
Via Elce di sotto, 8, 06123 Perugia (Italia)
and
Centro di Eccellenza SMAArt, c/o Dipartimento di Chimica,
Biologia e Biotecnologie, Università di Perugia
Via Elce di sotto, 8, 06123 Perugia (Italia)
S. Legrand, Dr. K. Janssens
AXES Research Group, Department of Physics,
Universiteit Antwerpen
Groenenborgerlaan 171, 2020 Antwerpen (Belgium)
Supporting information and the ORCID identification number(s) for the author(s) of this article can be found under: https://doi.org/10.1002/anie.201915490.

identify and map red lakes, especially eosin lake, in faded areas of paintings. Eosin pigments were used by van Gogh from 1888 to his death in 1890 and are prone to light-induced fading,[15–17] a phenomenon of which van Gogh was aware.[18] In letters he wrote to his brother during 1888–1890, he requested red lake tube paints, including *laque geranium* (geranium lake, known to contain eosin lake), *laque ordinaire* (ordinary lake), and *carmin* (carmine lake).[19] In 1889, van Gogh described one of the works containing red lake pigments, *The Olive Orchard*, in the collection of the National Gallery of Art (Washington, D.C.) in a letter to his brother as "…the field is violet and further away yellow ochre, the olive trees with bronze trunks have gray-green foliage, the sky is entirely pink, and 3 small figures pink also."[20] Comparison of van Gogh's description with a color image of the painting as it appears today (Figure 1) shows the pinks of the figures likely have faded, as well as portions of the background.

Even in faded regions, a low concentration of non-degraded colorants likely remains, the fluorescence spectra of which should be identifiable. First, a hyperspectral procedure to correct molecular fluorescence emission spectra for self-absorption was established. Second, the impact of fluorescence quenching and the presence of degradation products on the sensitivity of fluorescence imaging spectroscopy was assessed. Third, the method's sensitivity was compared to mapping methods based on Vis-NIR reflectance and XRF. Fourth, the three imaging modalities were compared in their ability to identify and map eosin lake and other lake pigments in van Gogh's *The Olive Orchard*.

Figure 1. Color image of *The Olive Orchard*. Vincent van Gogh, 1889, Chester Dale Collection, National Gallery of Art, Washington, D.C.

Results

Eosin Lake Reference Panels

The first reference panel (Figure 2A) consisted of paint-outs of eosin lake (eosin-Y complexed with lead, labeled eoPb)[21] mixed with zinc or lead white in varying concentrations. Results with zinc or lead white were similar, and only the lead white results are shown. A second set of reference panels consisted of eoPb mixed with one of several white pigments, of which one panel in the set was artificially aged while the other was not. All reference panels were measured in reflectance and molecular fluorescence mode with a high sensitivity Vis-NIR imaging spectrometer (400–950 nm,

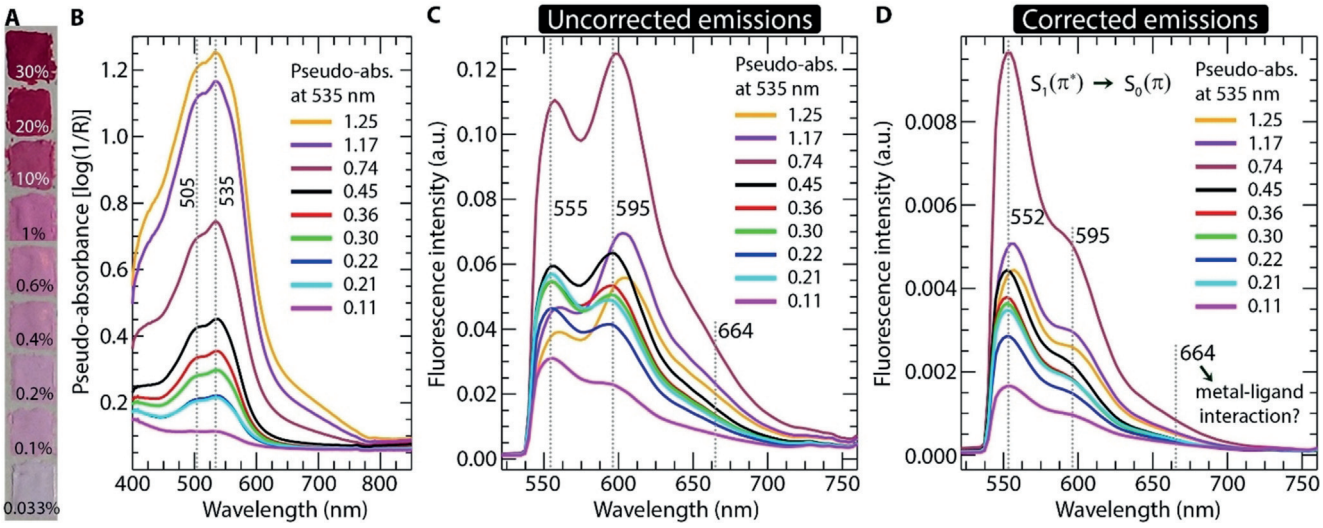

Figure 2. Pseudo-absorbance and fluorescence spectra of eosin lake reference paints. A) Visible image of eosin lake mixed with lead white reference paints. The concentration of eosin lake (eoPb) was varied, and the mass percent of eoPb to lead white that were intended are listed. B) Pseudo-absorbance spectra. The pseudo-absorbance maximum value provides a more accurate measure of the eosin lake concentration. C) Fluorescence spectra (approximately 480–525 nm excitation) before applying self-absorption correction. D) Fluorescence spectra after correction for effects of self-absorption. All spectra shown are an average of each paint sample (1600–2500 pixels).

2.5 nm spectral sampling). For fluorescence measurements, a broad band excitation source (approximately 480–525 nm) was used instead of a laser. An emission longpass filter (533–1000 nm) also was used to collect the molecular fluorescence. The reflectance and molecular fluorescence image cubes were spatially registered to one another,[22] and random noise in the spectral dimension was removed by principal component filtering. The procedure to correct molecular fluorescence image cube data for self-absorption was adapted from an algorithm for spectra collected with a non-imaging spectrometer[23] and a single wavelength excitation source[13,14] (see the Supporting Information for details).

To assess the success of the hyperspectral self-absorption correction procedure, a comparison to fluorescence spectra from a point spectrometer (Supporting Information, Figure S1) was made. The pseudo-absorbance spectra (log(1/reflectance), Figure 2B) of the paint samples in the concentration reference panel show the characteristic absorption features of eosin lake near 500 and 535 nm, and show the same absorption features at eoPb concentrations of 30% and below (above 30%, the spectra are saturated near 500–530 nm due to high concentration). The corresponding molecular fluorescence spectra from the same spatial pixel before and after correction (Figure 2C,D) show the same behavior as the single point fluorescence spectra. The uncorrected emission spectra at higher concentrations show the effect of self-absorption, in which the band near 590 nm (observed at 595 nm) is more intense than the band near 550 nm (observed at 555 nm). Upon correction for self-absorption, the molecular fluorescence spectra display the spectral characteristics of eosin lake, where the most intense emission occurs near 550 nm, with shoulders of decreasing intensity at approximately 590 and 665 nm.

A plot of the molecular emission peak intensity as a function of eoPb concentration (Figure 3A) shows a relatively linear increase in fluorescence up to approximately 1–10%, followed by a decrease in emission intensity for concentrations greater than 10%. Even though the eoPb emission intensity is quenched at higher concentrations, the shape of the corrected emission spectra is the same (Figure 3A inset) for all concentrations.

XRF imaging spectroscopy of the concentration reference panel was conducted using an in-house assembled system at an integration time approximately 10× longer than typical when using a commercial system to ensure spectra with higher signal to noise. In Figure 3B, the Br-K_α signal, defined as the area under the Br-K_α peak in an average XRF spectrum from each paint swatch (approximately 80 pixels), is plotted against the mass % of eosin lake. For the range of concentrations examined, Br was detected at an eosin concentration of greater than or equal to 1%. The detection limit for Br was calculated to be approximately 0.7–0.8 mass % of eosin (in lead white) for the experimental conditions used. With increasing eosin lake concentrations greater than or equal to 1%, the net Br-K_α intensity increases approximately linearly.

The second reference panel was used to explore the potential of fluorescence imaging spectroscopy to detect intact eosin in aged paintings. As shown in Figure 4, the corrected spectra before and after artificial aging have the same spectral shape that is consistent with the presence of intact eosin. No degradation products of eosin lake that absorb (approximately 480–525 nm) and emit in the visible spectral region have been observed.[24]

Molecular Fluorescence Imaging Spectroscopy to Identify and Map Eosin Lake within The Olive Orchard

A detail was imaged from van Gogh's *The Olive Orchard* that depicts one woman in a green dress standing on a ladder among the olive trees, and one woman beside the ladder, wearing what currently appears to be a white blouse and light pinkish skirt. A similar collection procedure and correction for self-absorption as that used for the eosin reference panels was followed.

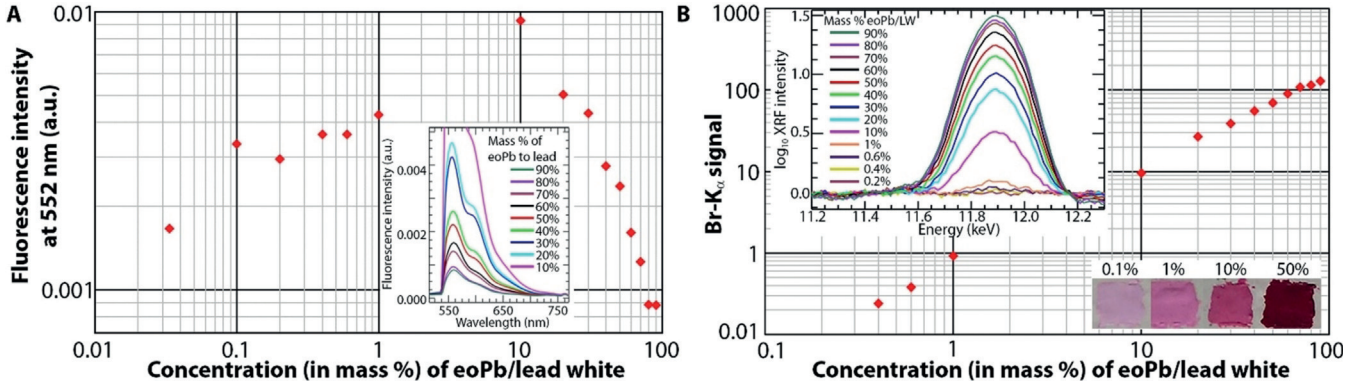

Figure 3. Molecular fluorescence detection of eosin lake (mixed into lead white) in comparison to XRF sensitivity to Br. A) The molecular fluorescence intensity linearly increases with eoPb concentrations up to approximately 1–10% after which it decreases, indicating that quenching is occurring. The emission spectral shape remains unchanged from low to high concentrations (inset) indicating no new fluorescent state is formed at high concentrations. B) At eoPb concentrations greater than or equal to 1%, Br-K_α signals increase approximately linearly, derived from the area below the Br-K_α peak determined by fitting the XRF spectra with a Gaussian. The inset shows the $\log_{10}$ of the average XRF spectrum from each paint swatch (approximately 80 pixels) after baseline subtraction (baseline approximated by a median filtered ($n=5$) log spectrum in which no significant Br-K_α peak was visible (0.1%)). Selected paint swatches demonstrate the color range.

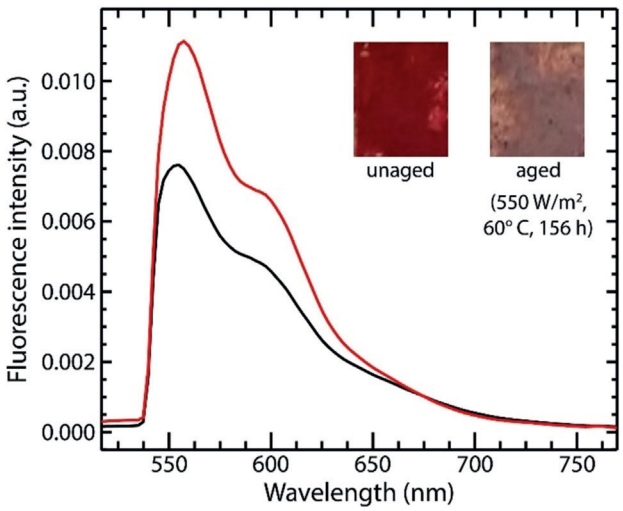

Figure 4. Molecular fluorescence spectra from unaged (red) vs. aged (black) eosin lake reference paints. The mass percent of eosin lake to lead white is 50%.

Many of the pigments in the area imaged can be determined from reflectance and XRF imaging spectroscopies, and this knowledge is useful when interpreting the molecular fluorescence spectra. Selected pigment maps from these two modalities are given in Figure S2 (reflectance) and Figure S3 (XRF) of the Supporting Information. In summary, the predominant pigments used include emerald green, viridian green, cobalt blue, Prussian blue, zinc white, yellow ochre, and vermilion. A red lake appears to be used in the dark outline of the woman, ladder, and tree.

Examination of the corrected molecular fluorescence image cube revealed emission spectra having bands between approximately 560 to 610 nm with full widths at half maximum of approximately 100 nm, along with shoulders that varied in position. Broad and varying emission spectra suggested that, in addition to fluorescence from red lake pigments, other sources of fluorescence were also collected, possibly from degradation products associated with the paint binder and pigments. As noted earlier, no degradation products of eosin lake have been observed to absorb (approximately 480–525 nm) and emit in the visible spectral region.[24] To minimize these broadly varying spectral features and enhance the presence of weak spectral features like those of eosin lake, the first derivative with respect to wavelength was calculated. Convex geometry methods (see the Supporting Information for details) were used to find first derivative spectra that represent a basis set of spectra that describe the scene, known as endmember spectra.

Five first derivative endmember spectra were recovered, three of which are spectrally similar and shown in Figure 5 A, along with their corresponding molecular fluorescence spectra. Each fluorescence spectrum displays similar spectral features with an emission maximum near 580–585 nm and a shoulder at approximately 665 nm (observed at 668 nm and like the spectra from the eosin lake reference panel), with the biggest distinction among them only being the difference in their fluorescence intensity. The fluorescence shoulder near 665 nm is seen in the first derivative spectra as a sharp change in slope, marked with a vertical dashed line. The map shown in Figure 5 B displays the distributions of the red-, purple-, and blue-colored first derivative endmember spectra and includes the pinkish-gray blouse covering the breast of the woman and along the edge of her back, some light purple-grayish strokes in the background, and the dark outline of the woman's hair. These areas indicate where non-degraded eosin lake is likely present. In Figure 5 C, the elemental Br map

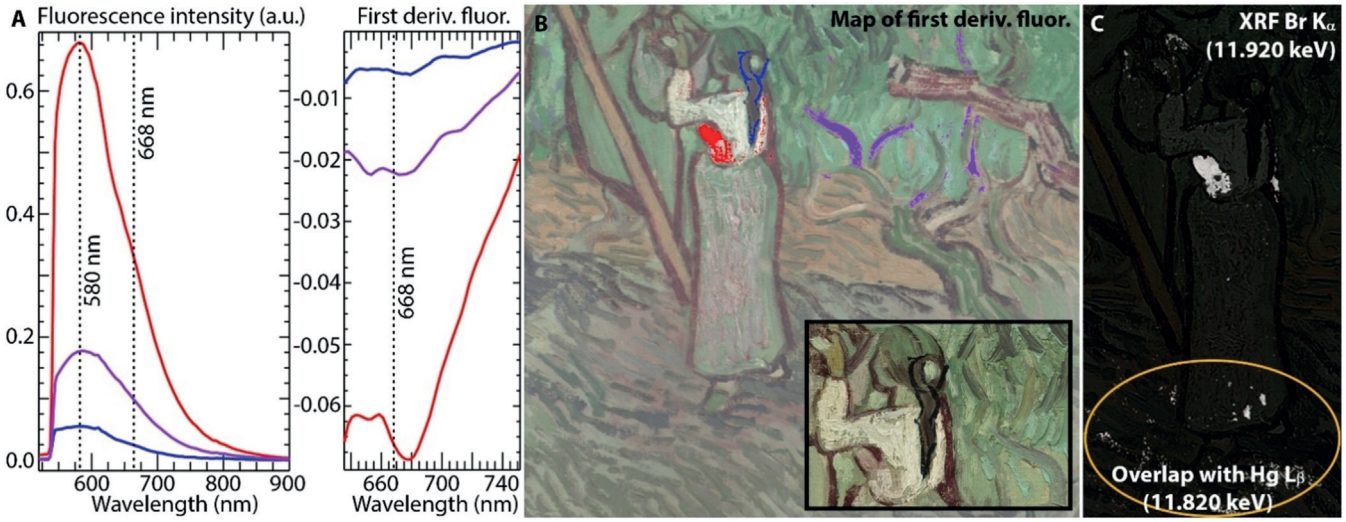

Figure 5. Spectra and maps indicating presence of eosin lake. A) First derivative endmember spectra and the corresponding molecular fluorescence spectra. Eosin-containing regions are indicated by the approximately 665 nm emission (observed here at 668 nm) in fluorescence spectra and corresponding inflection point in first derivative spectra. B) Map of first derivative endmember spectra (635–750 nm) with color detail (inset). C) Log intensity of the XRF Br map. Overlap with Hg emission denoted with yellow circle (see also Figure S3 in the Supporting Information).

from XRF imaging spectroscopy shows a concentration of Br near the woman's breast and also at one site along the edge of her back.

Molecular Fluorescence Imaging Spectroscopy to Identify and Map Other Red Lake Pigments within The Olive Orchard

Of the five recovered first derivative endmember spectra, the two that were not characteristic of eosin were used to map two other red lake pigments (Figure 6A, right). The associated reflectance and molecular fluorescence spectra from the endmember spatial pixels are shown at the left and middle in Figure 6A. The maroon reflectance spectrum is characterized by absorption sub-bands near 520 and 557 nm with a broad increase at red wavelengths. Furthermore, the fluorescence maximum of this red lake is shifted to longer wavelengths (600 nm) relative to the maxima seen in Figure 5A (580–585 nm), another indication that the material is different from eosin lake. The maroon first derivative endmember maps to part of the outline of the woman's skirt, blouse, and sleeve, as well as to the outline of the ladder and a tree trunk on the right (Figure 6B). These regions on the painting are a very dark maroon color, as can be seen in the inset in Figure 6B. The other red lake is characterized by the green reflectance spectrum having absorption sub-bands at 545, 577, and 623 nm. The green corresponding fluorescence spectrum shows an emission maximum near 575 nm, and its first derivative shows an inflection point near 648 nm (but not near 665 nm). The green endmember maps to the outline of the woman's feet and some strokes along the ground, all appearing blue-gray (Figure 6B).

The regions mapped by the first derivative spectra also correlate with the presence of particular chemical elements. The XRF scatter plot (Figure 6C) shows the intensity (in counts) of Ca K_α (3.69 keV) versus Sn L_α (3.44 keV) for each spatial pixel in the XRF maps. Pixels with XRF spectra showing high counts of Ca and zero or low counts of Sn are colored maroon, and they map to similar regions as the first derivative maroon endmember, including the outline of the woman and the ladder. Pixels with high counts of both Ca and Sn are colored green, and they map to similar regions as the green first derivative endmember, in addition to the woman's hair down her back, and some paint strokes near her hands at the top of the map.

Discussion

Eosin Lake Reference Panels

Because the spectral distribution of molecular fluorescence emitted by eosin lakes overlaps the region where they also absorb, uncorrected fluorescence spectra can show the effects of self-absorption, even at modest concentrations (1%, Figure 2C). Once corrected for self-absorption, the molecular fluorescence emission spectra collected with either laser illumination (Supporting Information, Figure S1) or broadband illumination (Figures 2D and 3A inset) all exhibit

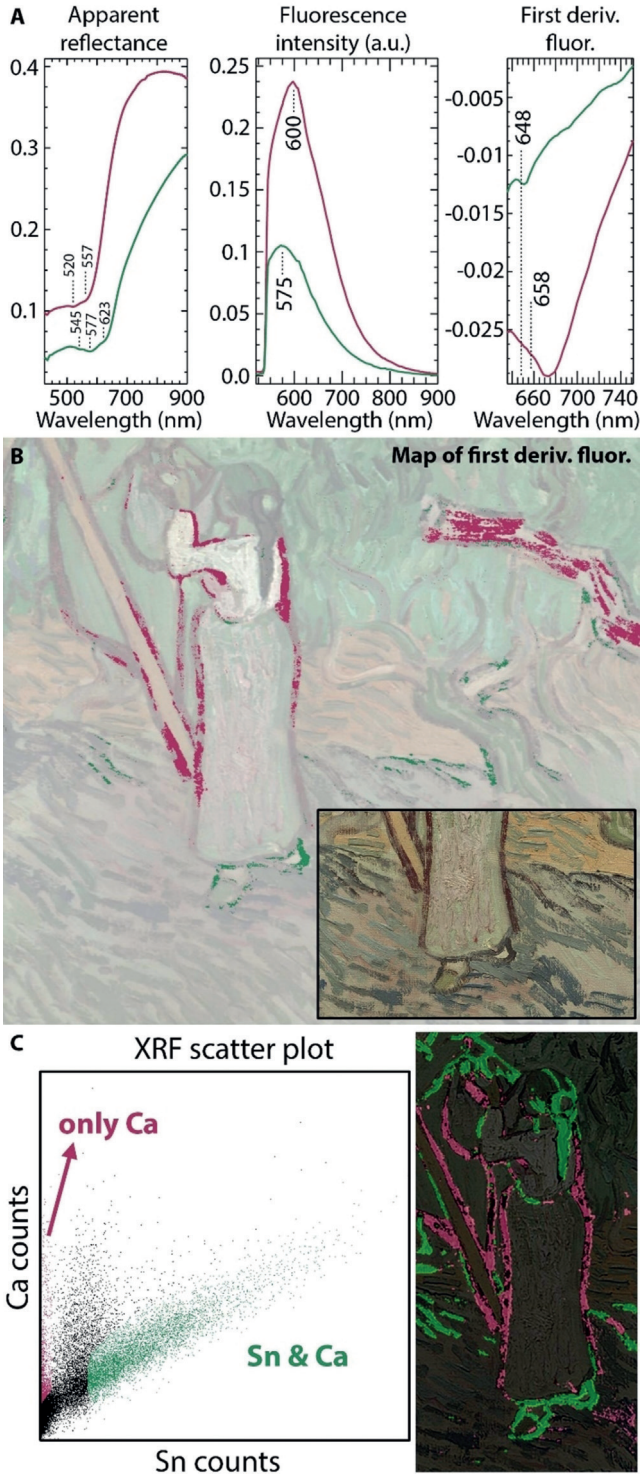

Figure 6. Spectra and maps indicating the presence of two additional red lake pigments. A) First derivative endmember spectra are shown at right, in conjunction with the average reflectance and molecular fluorescence spectra of the same pixels used to define the derivative endmembers. B) Map of first derivative endmember spectra (635–750 nm) with color detail (inset). C) XRF scatter plot and corresponding map showing areas that have XRF spectra with calcium (maroon pixels) or both tin and calcium (green pixels). The Ca K_α peak at 3.69 keV and Sn L_α peak at 3.44 keV are used in the scatter plot.

spectral features intrinsic to eosin lake: an emission maximum near 550 nm, with shoulders of decreasing intensity near 590 and 665 nm. The bands centered near 550 and 590 nm have been assigned to the $S_1(\pi^*)\rightarrow S_0(\pi)$ emission with the lower energy 590 nm shoulder resulting from a transition to a vibrational level within the electronic ground state.[25] The band centered near 665 nm possibly results from an interaction between the metal substrate and the ligand.

For eoPb concentrations greater than 10%, the fluorescence intensity decreased with increasing concentration (Figure 3A). This trend is indicative of dynamic quenching processes, such as energy transfer, which has been observed for dyes in solution.[26] In contrast, if static quenching is the reason for the decrease in the observed fluorescence, one would expect to see a different absorption spectrum due to strong coupling in the ground state that alters the electronic properties of the red lake. However, inspection of the absorption spectra at different eoPb concentrations shows no new absorption bands (Figure 2B), and the corrected fluorescence spectra show the emission features expected for eosin lake (Figure 3A inset).

In the artificially aged reference panel, degradation using ultraviolet and/or visible light does produce some photoproducts that absorb UV and deep blue light ($\lambda < 425$ nm).[24] Although the number and structure of the resulting degradation products of eosin lake have yet to be elucidated, they do not absorb the light from approximately 480–525 nm used here so they cannot produce a fluorescence contribution. Importantly, the corrected fluorescence spectra show the characteristic emission features of eosin lake, regardless of whether the sample was aged (Figure 4).

Both molecular fluorescence and reflectance imaging spectroscopy could detect eosin lake in the presence of a white pigment, even at the lowest concentrations prepared (approximately 0.033%, Figure 2), and thus the detection limit of these respective techniques was not reached. With reflectance spectroscopy, white pigments cause increased light scattering within the paint volume and increase the chance for detection of the red lake.[27] With XRF imaging spectroscopy, Br was clearly detected at an eosin lake concentration of 1% by mass but was not detected at the lowest concentrations prepared, even though these paint samples are visibly pink. This is likely because eosin is present in a mixture with lead or zinc white paint. Bromine emits X-ray fluorescence (Br-K_α at 11.92 keV; Br-K_β at 13.29 keV) in the region where the absorption edges of lead (Pb-L_3 absorption edge at 13.03 keV) and zinc (Zn K-absorption edge at 9.65 keV) are present, such that a substantial part of the primary radiation required to induce emission of Br-K radiation (namely, with energy above that of the Br-K edge at 13.47 keV) becomes absorbed while a significant part of the XRF that is effectively emitted by Br never leaves the paint in which it is generated. In order to increase the detection limit to approximately 0.1%, either the measurement time would have to be increased by 100× (333 ms to 33 s) or a 10×10 pixel area could be summed. This is impractical when imaging with the conditions employed here. However, if the eosin lake is applied as a thin glaze on the surface such that the Br XRF emission is not absorbed by dense (white) paint, then likely XRF imaging spectroscopy could detect it at lower concentration levels.

Evidence for Eosin Lake Pigment in The Olive Orchard

The molecular fluorescence spectra from *The Olive Orchard* (Figure 5A) display a shoulder near 665 nm like in the eosin lake reference paints. The most intense spectrum exhibiting the 665 nm shoulder was present in the blouse of the woman, near her breast, represented by the red endmember spectrum (Figure 5B). The breast of the woman contains Zn, Pb, and Br (Figure 5C). The presence of Br, diagnostic of eosin, provided independent confirmation that the spectral feature near 665 nm in the fluorescence and first derivative spectra is likely a good marker to use for eosin lakes where pigment mixtures are present. The current light pink appearance of the woman's breast is in the same approximate color range of paints from the eosin lake concentration reference panel containing less than 1% eosin lake by mass. However, in the assumption that the pink paint layers in the woman's breast and in the test panel are of comparable thickness, then the recorded XRF Br signal corresponds to an eosin lake concentration of approximately 10%; lead white mixed with 10% eosin lake has a deeper pink color (Figure 3B inset). Prior research on samples has shown that eosin lake in van Gogh paintings from this time period are associated with paint tubes he ordered by the name *laque geranium*,[15] which is most likely the source of eosin lake detected in *The Olive Orchard*.

The purple- and blue-colored endmember in Figure 5A both display the spectral feature at approximately 665 nm. The purple-colored endmember maps to some light purple-gray strokes in the background (see Figure 5B inset for current color appearance) that contain a mixture of pigments, including viridian based on the reflectance spectra, confirmed by the chromium XRF map (see the Supporting Information for details). The presence of zinc white and emerald green were also inferred based on the zinc, copper, and arsenic XRF maps. The light purple-gray appearance likely results from the green pigments and eosin lake that has faded, although not completely since the spectral feature near 665 nm was detected.

The blue-colored endmember has a low emitted fluorescence intensity and maps to the dark outline of the woman's hair, whose predominant color is due to Prussian blue based on the iron and potassium distribution in the XRF maps and the outline's low reflectance from 400–1000 nm.[28] Prior studies found van Gogh used eosin lake with blue pigments, including Prussian blue, to paint contours,[15,29] so the current finding is consistent with this practice. Interestingly, XRF imaging spectroscopy did not detect Br in either the light purple-grayish background strokes (one of these strokes was included at the far-right edge of the area scanned) or the dark blue outline of the woman's hair. Because the same fluorescence profile was observed in all three endmember spectra, and the XRF detection of Br was validated on the breast region, this suggests that molecular fluorescence spectroscopy can detect lower quantities of eosin lake in pigment mixtures

containing zinc white, copper and chrome green pigments, and Prussian blue than XRF spectroscopy. Fluorescence spectroscopy also outperformed reflectance spectroscopy in detecting eosin lake because the visible reflectance spectra were dominated by spectral features from pigments that strongly influenced the color in these regions.

Evidence for Other Red Lake Pigments in The Olive Orchard

Two additional fluorescent red lake pigments were identified and mapped using the first derivative spectral endmembers (Figure 6A, right). This is not surprising as van Gogh used multiple red lake pigments within single paintings from this time period.[30] The maroon-colored derivative endmember mapped to fluorescent areas, including the maroon outline of the woman and ladder and a tree trunk on the right (Figure 6B). The corresponding reflectance spectrum of this endmember (Figure 6A, left) shows absorption sub-bands near 520 and 557 nm, characteristic of insect-based red lakes[6,31] and due to the $S_0(\pi)\rightarrow S_1(\pi^*)$ electronic transition.[25] The associated molecular fluorescence spectrum (Figure 6A, middle) has an emission maximum near 600 nm, which is red-shifted relative to that seen for the eosin lake used in the breast of the woman (580 nm) but not quite as shifted as in a prior study where the corrected emission maxima of insect-based red lakes in solid paint samples occurred between 615–630 nm.[31] This discrepancy may be from the presence of some eosin lake, as suggested by the inflection point in the first derivative spectra at 658 nm and the XRF detection of Br in the maroon outline near the woman's waist (Figure 5C). The maroon outline of the ladder and woman's torso is also associated with the element Ca (Figure 6C).

The green-colored derivative endmember mapped to the outline of the woman's feet and some strokes along the ground, all of which appear predominately dark gray-blue, but close visual inspection shows layering and mixing with a deep red pigment (Figure 6B). The associated reflectance spectrum has absorption bands at 545, 577, and 623 nm characteristic of d–d electronic transitions of the cobalt(II) ion in cobalt blue.[32] Other cobalt pigments were ruled out because cerulean blue, $CoO{\cdot}n\,SnO_2$, and cobalt violet, $Co_3(PO_4)_2$ or $Co_3(AsO_4)_2$, have visible and NIR absorption bands that are shifted relative to cobalt blue. The corresponding fluorescence emission maxima occurs near 575 nm. Because cobalt blue itself does not fluoresce, an emitting pigment must be painted on top of or mixed in with cobalt blue, but it cannot be identified without additional information. The XRF maps showed that the likely red lake is associated with Sn and Ca (green pixels, Figure 6C). The Sn- and Ca-containing pixels are also found in places where cobalt blue is not present or at a much lower concentration. Such areas appear brownish in the relatively pure red lake paint strokes near the woman's hands, and also in the hair down her back that contains an admixture/layering with green pigments. The fact that Sn was found here without Co suggests its presence is due to the red lake and not cerulean blue. Furthermore, prior analysis by Geldof et al. of 59 van Gogh paintings completed during the last two years of his life showed he did not use cerulean blue during this time.[30] Researchers also noted that he used red lake pigments on their own or in mixtures with blue and green pigments,[15,30] and that Al, Sn, and Ca were associated with the substrates of organic red lake pigments. In general, when they identified cochineal it was on a substrate containing Al and Ca, which was linked to paint van Gogh ordered by the name *laque ordinaire.* When both cochineal and redwood were identified, they were on a substrate containing Al and Sn, which was linked to *carmin.* The cochineal and redwood paint also possibly contained calcium carbonate.

The results from *The Olive Orchard* are consistent with this prior research. The maroon pixels in Figure 6 show an insect-based red lake, possibly cochineal, is affiliated with Ca, and this deep maroon-colored paint is likely the *laque ordinaire* paint. The green pixels in Figure 6 show a brownish-colored red lake is associated with Sn and Ca, possibly the *carmin* paint if indeed it contained calcium carbonate or it may be a mixture of the Ca-containing *laque ordinaire* and the Sn-containing *carmin.* Because these red lake pigments map to discrete areas, this suggests that van Gogh used different tube paints based on color or mixed the paints with different pigments (namely, cobalt blue) to create the desired color.

Conclusion

By inducing the $S_0(\pi)\rightarrow S_1(\pi^*)$ transition directly and correcting for self-absorption, the fluorescence spectral features of eosin lake could be identified, even at high concentrations when the emission intensity was quenched or in aged samples. Molecular fluorescence imaging spectroscopy was used to identify and map low concentrations of residual eosin lake in faded areas of van Gogh's *The Olive Orchard*, even in the presence of pigment mixtures and layering. The distribution of eosin lake enabled visualizing how van Gogh used it, likely from the tube paint *laque geranium.* Even when the fluorescence spectra alone do not support a conclusive identification, the ability to map a fluorescent component is useful, particularly when paired with other imaging spectroscopies. These results demonstrate that high sensitivity, molecular fluorescence imaging spectroscopy is a new imaging modality that can complement XRF and reflectance imaging spectroscopies to study fugitive red lake pigments.

Acknowledgements

We thank Damon Conover and Roxanne Radpour for help with the fluorescence self-absorption correction, and Ella Hendricks for discussions about van Gogh's letters and materials. K.J. and S.L. thank the Research Council of the University of Antwerp for financial support (ID grant 25805 to S.L. and GOA project SolarPaint). Also FWO, Brussels provided financial support (grants G056619N and G054719N). The European research project IPERION-CH, funded by the European Commission, H2020-INFRAIA-2014-2015 (Grant agreement n. 654028) is also acknowledged.

Conflict of interest

The authors declare no conflict of interest.

Keywords: analytical methods · eosin lake pigment · fluorescence spectroscopy · heritage science · X-ray fluorescence

How to cite: *Angew. Chem. Int. Ed.* **2020**, *59*, 6046 – 6053
Angew. Chem. **2020**, *132*, 6102 – 6109

[1] J. Kirby in *Art of the past, sources and reconstructions* (Ed.: M. Clarke, J. H. Townsend, A. Stijnman), Archetype Publications, London, **2005**, pp. 69 – 77.
[2] J. Kirby, M. Spring, C. Higgitt, *National Gallery Technical Bulletin* **2005**, *26*, 71 – 87.
[3] J. Kirby, M. Spring, C. Higgitt, *National Gallery Technical Bulletin* **2007**, *28*, 69 – 95.
[4] J. Wouters, C. M. Grzywacz, A. Claro, *Stud. Conserv.* **2011**, *56*, 231 – 249.
[5] F. Sabatini, A. Lluveras-Tenorio, I. Degano, S. Kuckova, I. Krizova, M. P. Colombini, *J. Am. Soc. Mass Spectrom.* **2016**, *27*, 1824 – 1834.
[6] C. Bisulca, M. Picollo, M. Bacci, D. Kunzelman in *9th International Conference on NDT of Art*, Jerusalem, Israel, **2008**.
[7] M. J. Melo, P. Nabais, M. Guimarães, R. Araújo, R. Castro, M. C. Oliveira, I. Whitworth, *Philos. Trans. R. Soc. London Ser. A* **2016**, *374*, 20160050.
[8] A. Romani, C. Clementi, C. Miliani, G. Favaro, *Acc. Chem. Res.* **2010**, *43*, 837 – 846.
[9] E. R. de la Rie, *Stud. Conserv.* **1982**, *27*, 65 – 69.
[10] E. R. de la Rie, *Stud. Conserv.* **1982**, *27*, 102 – 108.
[11] M. G. Lagorio, L. E. Dicelio, M. I. Litter, E. San Román, *J. Chem. Soc. Faraday Trans.* **1998**, *94*, 419 – 425.
[12] M. E. Ramos, M. G. Lagorio, *Photochem. Photobiol. Sci.* **2004**, *3*, 1063 – 1066.
[13] C. Clementi, C. Miliani, G. Verri, S. Sotiropoulou, A. Romani, B. G. Brunetti, A. Sgamellotti, *Appl. Spectrosc.* **2009**, *63*, 1323 – 1330.
[14] G. Verri, C. Clementi, D. Comelli, S. Cather, F. Piqué, *Appl. Spectrosc.* **2008**, *62*, 1295 – 1302.
[15] M. Geldof, M. de Keijzer, M. van Bommel, K. Pilz, J. Salvant, H. van Keulen, L. Megens in *Van Gogh's Studio Practice* (Ed.: M. Vellekoop, M. Geldof, E. Hendriks, L. Jansen, A. de Tagle), Mercatorfonds, Brussels, **2013**, pp. 268 – 289.
[16] A. Burnstock, I. Lanfear, K. J. van den Berg, L. Carlyle, M. Clarke, E. Hendriks, J. Kirby, *ICOM-CC 14th triennial meeting preprints*, The Hague, **2005**, pp. 459 – 466.
[17] A. Alvarez-Martin, S. Trashin, M. Cuykx, A. Covaci, K. De Wael, K. Janssens, *Dyes Pigm.* **2017**, *145*, 376 – 384.
[18] E. Hendriks, *"Paintings fade like flowers": color change in paintings by Vincent van Gogh*, Archetype, London, in association with the ICON Paintings Group, **2016**.
[19] *Vincent van Gogh: The Letters*, Thames and Hudson, New York, **2009**.
[20] Letter 829, Saint-Rémy-de-Provence, dated on or about 19 December, **1889**, http://vangoghletters.org/vg/letters/let829/letter.html.
[21] C. Anselmi, D. Capitani, A. Tintaru, B. Doherty, A. Sgamellotti, C. Miliani, *Dyes Pigm.* **2017**, *140*, 297 – 311.
[22] D. M. Conover, J. K. Delaney, M. H. Loew, *Appl. Phys. A* **2015**, *119*, 1567 – 1575.
[23] A. Romani, C. Grazia, C. Anselmi, C. Miliani, B. G. Brunetti, *Proc. SPIE-Int. Soc. Opt. Eng.* **2011**, *8084*, 808403 – 808401.
[24] A. Chieli, Ph.D. Thesis, University of Perugia, **2018**.
[25] S. Daly, A. Kulesza, G. Knight, L. MacAleese, R. Antoine, P. Dugourd, *J. Phys. Chem. A* **2016**, *120*, 3484 – 3490.
[26] J. S. Bellin, *Photochem. Photobiol.* **1968**, *8*, 383 – 392.
[27] A. Alvarez-Martin, K. Janssens, *Microchem. J.* **2018**, *141*, 51 – 63.
[28] M. Bacci, D. Magrini, M. Picollo, M. Vervat, *J. Cult. Herit.* **2009**, *10*, 275 – 280.
[29] S. A. Centeno, C. Hale, F. Carò, A. Cesaratto, N. Shibayama, J. Delaney, K. Dooley, G. van der Snickt, K. Janssens, S. A. Stein, *Heritage Sci.* **2017**, *5*, 18.
[30] M. Geldof, L. Megens, J. Salvant in *Van Gogh's Studio Practice* (Ed.: M. Vellekoop, M. Geldof, E. Hendriks, L. Jansen, A. de Tagle), Mercatorfonds, Brussels, **2013**, pp. 238 – 255.
[31] C. Clementi, B. Doherty, P. L. Gentili, C. Miliani, A. Romani, B. G. Brunetti, A. Sgamellotti, *Appl. Phys. A* **2008**, *92*, 25 – 33.
[32] M. Bacci, M. Picollo, *Stud. Conserv.* **1996**, *41*, 136 – 144.

Manuscript received: December 4, 2019
Accepted manuscript online: January 21, 2020
Version of record online: February 11, 2020

